THIS ARTICLE IS BEING REPRINTED FROM *THE JOURNAL OF NUCLEAR MEDICINE*

Brain Amyloid Imaging*

Christopher C. Rowe and Victor L. Villemagne

Department of Nuclear Medicine and Centre for PET, Austin Health, Melbourne, Australia

Imaging of brain β-amyloid plaques with ^{18}F-labeled tracers for PET will likely be available in clinical practice to assist the diagnosis of Alzheimer disease (AD). With the rapidly growing prevalence of AD as the population ages, and the increasing emphasis on early diagnosis and treatment, brain amyloid imaging is set to become a widely performed investigation. All physicians reading PET scans will need to know the complex relationship between amyloid and cognitive decline, how to best acquire and display images for detection of amyloid, and how to recognize the patterns of tracer binding in AD and other causes of dementia. This article will provide nuclear medicine physicians with the background knowledge required for understanding this emerging investigation, including its appropriate use, and prepare them for practical training in scan interpretation.

Key Words: Alzheimer disease; β-amyloid; PET

J Nucl Med Technol 2013; 41:11–18
DOI: 10.2967/jnumed.110.076315

β-amyloid (Aβ) plaques are present in moderate to frequent numbers in the cortical gray matter in all cases of Alzheimer disease (AD) and develop many years before the onset of dementia. In contrast, Aβ plaques are not found in frontotemporal dementia or pure vascular dementia. Therefore, applications for amyloid imaging will include confirmation or exclusion of AD, differential diagnosis of dementia, particularly for the distinction of AD from frontotemporal dementia, and earlier diagnosis of AD. Although there is presently no effective treatment for AD—only symptomatic medication of modest effect—demand for earlier and more accurate diagnosis is growing. Clinicians and patients and their families are increasingly seeking more accurate diagnostic and prognostic information. Researchers want to trial potential therapies earlier before patients have dementia, when the therapies are more likely to be beneficial. Clinical diagnosis alone has only moderate accuracy and requires the presence of dementia, but specific biomarkers, such as amyloid imaging, for AD-related pathologic changes will allow more accurate diagnosis and earlier diagnosis when patients are only mildly symptomatic.

The first PET tracer specific for Aβ plaques was developed by Chet Mathis and William Klunk at the University of Pittsburgh through modification of thioflavin T, a fluorescent dye used by pathologists to identify plaques in brain tissue specimens (*1,2*). The radiopharmaceutical was labeled with ^{11}C, and the first human studies were commenced in 2002 through a collaboration with Uppsala University, Sweden, where the compound was given the name Pittsburgh compound B (^{11}C-PiB). After publication of this study in 2004 (*3*), ^{11}C-PiB imaging spread rapidly to academic centers worldwide. Recognizing the need for an amyloid tracer labeled with ^{18}F, several groups soon embarked on development programs, and in 2008 the first report of successful imaging in humans with an ^{18}F-labeled amyloid tracer appeared (*4*). Subsequently, 3 companies have progressed ^{18}F-labeled amyloid tracers through clinical development programs. These tracers are florbetapir (previously known as AV-45) (*5,6*), flutemetamol (*7*), and florbetaben (previously known as AV-1) (*4,8,9*). Although ^{11}C-PiB PET images in AD usually show binding in gray matter in excess of that in white matter, this is not the case for the ^{18}F-labeled tracers that will be the mainstay of clinical practice. All ^{18}F-labeled tracers currently in late phases of clinical development have high nonspecific white matter uptake giving a distinctive white matter pattern in scans of healthy subjects. In AD, the ^{18}F-labeled tracers frequently show loss of the gray matter–white matter demarcation and consequent loss of the normal white matter pattern as the predominant evidence of cortical amyloid plaque and less often show the clearly intense binding in the cortical ribbon typical of a positive ^{11}C-PiB scan.

AD AND DEMENTIA

Clinical Characteristics of Dementia

Dementia is defined as cognitive impairment of sufficient severity that it prevents independent function in the patient's usual occupation or daily activities. There are many causes for cognitive impairment, but the most common in the elderly is neurodegenerative disease. Metabolic problems such as hypothyroidism, severe vitamin B12 deficiency, chronic hypoxia, major organ failure, autoimmune encephalopathy,

Received May 25, 2011; revision accepted Aug. 17, 2011.
For correspondence or reprints contact: Christopher C. Rowe, Department of Nuclear Medicine and Centre for PET, Austin Health, Heidelberg, Victoria 3084, Australia.
E-mail: christopher.rowe@austin.org.au
*NOTE: FOR CE CREDIT, YOU CAN ACCESS THIS ACTIVITY THROUGH THE SNMMI WEB SITE (http://www.snmmi.org/ce_online) THROUGH MARCH 2015. PARTICIPANTS WHO HAVE ALREADY TAKEN THE EXAM USING *JNM* AND PASSED CANNOT RETAKE THE EXAM.
Published online Feb. 8, 2013.

stroke, normal-pressure hydrocephalus, and subdural hematoma need to be excluded but account for less than 5% of presentations with progressive cognitive decline. The most common cause of neurodegenerative disease in the older population is AD, and this accounts for about 70% of cases of dementia. Less common causes include dementia with Lewy bodies (about 15%), frontotemporal dementia (more common in late middle age and the younger elderly), and vascular dementia. Infrequent conditions include mesial temporal sclerosis (usually found in the very elderly), nonspecific tauopathy, and argyrophilic grain disease (*10*). Vascular disease frequently accompanies neurodegenerative conditions, and cases with multiple types of neuropathology are not uncommon.

AD is an irreversible, progressive neurodegenerative disorder clinically characterized by memory loss and other cognitive and functional decline. It leads invariably to death, usually within 7–10 y of diagnosis. Symptoms usually precede diagnosis by several years, and longitudinal studies of older populations have found a subtle decline in cognition up to 10 y before dementia. AD not only has devastating effects on the patients and their caregivers but also has a tremendous socioeconomic impact on families and the health system, a burden that will only increase in the upcoming years as the population of most countries ages (*11*). The prevalence of AD is age-dependent, affecting 1% of the population at age 60 y and then doubling every 5 y, with the result that 25% of persons aged 85 y have the disease.

At this point there is no cure for AD, nor is there a proven way to slow the rate of neurodegeneration. Symptomatic treatment with an acetylcholinesterase inhibitor (donepezil, galantamine, rivastigmine) or a glutamatergic moderator (memantine) provides modest benefit in some patients, usually by temporary stabilization rather than a noticeable improvement in memory function. Amyloid imaging with PET is contributing to the development of more effective therapies by allowing better selection of patients for antiamyloid therapy trials and providing a means to measure the impact of these therapies on brain amyloid load (*12*).

Pathology of AD

The typical end-stage macroscopic pathologic picture of AD is gross cortical atrophy, whereas microscopically, there is widespread cellular degeneration and the presence of the pathologic hallmarks of the disease: intracellular neurofibrillary tangles and extracellular amyloid plaques (*13,14*). In earlier stages, the atrophy is predominantly seen on MRI in the hippocampi and adjacent mesial temporal regions, and with volumetric voxel-based MRI techniques, atrophy is also found in the posteromedial parietal lobe (precuneus and posterior cingulate gyrus) and lateral temporal lobe cortex. Amyloid plaques are most abundant in the frontal cortex—particularly the orbital and medial frontal areas—and in the cingulate gyrus, precuneus, and lateral parietal and temporal regions. There are relatively fewer plaques in the primary sensorimotor and occipital cortex and the mesial temporal areas, in contrast to neurofibrillary tangles, which are present in highest density in the mesial temporal areas, including the hippocampi (*15,16*).

Aβ plaques may be either diffuse or dense. Diffuse plaque is assumed to be an early phase of plaque formation. Dense plaques may be described as compact, dense, or cored and are called neuritic when associated with local neuronal damage and inflammation. Dense plaque is characteristic of AD. The PET amyloid tracers developed to date have low affinity for diffuse plaque, and scans may be negative when only diffuse plaque is present. The distribution and density of Aβ plaques, measured postmortem, have not been consistently shown to correlate with the degree of cognitive impairment in AD. The best correlation has been observed with neurofibrillary tangles and soluble levels of Aβ (*17–19*). These soluble forms of Aβ, in equilibrium with the insoluble Aβ in plaques, are neurotoxic through several possible mechanisms, including oxidative stress, excitotoxicity, energy depletion, toxic oxidative interaction with various metal species, inflammatory response, and apoptosis. Nevertheless, the exact mechanism by which Aβ might produce synaptic loss and neuronal death is still controversial (*20*).

To date, most evidence supports the notion that the breakdown of normal Aβ handling is central to AD pathogenesis. Compelling genetic data support this Aβ-centric theory (*21,22*). To date, 3 gene mutations have been linked to autosomal dominant, early-onset familial AD. These are the genes for amyloid precursor protein, presenilin 1, and presenilin 2. The ε4 allele of apolipoprotein E is strongly implicated in late-onset sporadic AD. All these genes influence Aβ handling, either by increased production or reduced clearance (*23*).

The Changing Approach to Diagnosis of AD

The criteria for clinical diagnosis of AD were described in 1984 and rely on establishing the presence of progressive impairment in memory and in at least one other area of cognition such as language or visuoconstructional function while excluding other causes. To meet these clinical criteria for AD, the cognitive impairment must be of sufficient severity to cause dementia, that is, prevent individuals from undertaking their usual occupation or daily activities such as driving, cooking, or shopping (*24*). Structural brain imaging with CT or MRI and blood tests are done to exclude alternate causes of dementia such as normal-pressure hydrocephalus, hypothyroidism, and stroke. However, compared with postmortem histopathologic diagnosis, clinical diagnosis in most centers is only 80%–85% sensitive and 70% specific for AD (*25*). Other causes of dementia such as frontotemporal dementia and dementia with Lewy bodies have many features in common with AD and are frequently misdiagnosed as AD. Recently, the diagnostic criteria for AD have been revisited, and a new category,

"probable AD dementia with evidence of the AD pathophysiologic process," was created by the 2011 National Institute on Aging and Alzheimer Association workgroup (*26*). The group's recommendation states that biomarkers (such as amyloid imaging) may be useful in 3 circumstances: in investigational studies, in clinical trials, and as optional clinical tools for use when available and when deemed appropriate by the clinician.

The most validated biomarkers for AD fall under 2 categories: those that reflect the specific pathology of AD and those that reflect neuronal damage or dysfunction. The pathologic biomarkers of AD are Aβ imaging and cerebrospinal fluid assay of the amyloid peptide, $A\beta_{42}$. The latter is reduced in subjects with brain amyloid deposition for reasons that are not fully understood but are most likely due to trapping of the peptide in the plaques (*27–30*). The pathologic biomarkers are thought to be present before those biomarkers that reflect neuronal damage (*29*). The biomarkers for neuronal damage or dysfunction are atrophy on MRI, hypometabolism on ^{18}F-FDG PET, and elevation of cerebrospinal fluid tau protein. In MRI, the location of atrophy adds specificity for AD and is most prominent in the hippocampi and adjacent entorhinal cortex (*31–33*). In ^{18}F-FDG PET, the pattern of hypometabolism gives specificity for AD and is found in the lateral and medial posterior (precuneus) parietal cortex, lateral temporal cortex, and posterior cingulate gyrus (*34,35*). Although present in most cases of AD, tau and phospho-tau may be present for other reasons, including acute stroke, because they are released into cerebrospinal fluid from damaged neurons. Aβ imaging shows increased tracer binding in cortical areas known to have high concentrations of amyloid plaques (*3,36*).

Prodromal AD

Symptoms and milder degrees of cognitive impairment precede the dementia of AD by several years. This phase has been termed mild cognitive impairment (MCI) (*37,38*), but advances in biomarkers for AD have recently led to proposals for more definitive diagnoses such as "prodromal AD" by the International Working Party for New Research Criteria for the Diagnosis of AD (*39*) or "MCI due to AD" by the National Institute for Aging and Alzheimer Association workgroup (*40*). The recommendations of the National Institute on Aging and Alzheimer's Association define MCI due to AD as "high likelihood" when both an amyloid and a neurodegenerative biomarker are positive for AD, as "intermediate likelihood" if just one biomarker is tested and that is positive, or as MCI "unlikely due to AD" if both amyloid and neurodegenerative biomarkers are negative. These diagnoses cannot be made on clinical grounds alone, as patients with MCI proceed to other types of dementia in 20% of cases or do not progress to dementia at all in 30%–40% of cases (*38,41,42*). Delaying diagnosis in a symptomatic person until dementia is apparent results in uncertainty and frustration for the patient and the family, costly serial investigations, and delay in potentially beneficial symptomatic therapy. Alternatively, commencing therapy in MCI without other evidence to support the presence of prodromal AD will lead to inappropriate medication use in about 50% of cases. An emerging reason for earlier and more accurate diagnosis of AD is that disease-modifying therapies currently under development are more likely to be effective at slowing or halting disease progression if given early, before dementia and extensive neuronal death have developed.

AD Pathology in Healthy Elderly

AD-related neuropathology is also found in about 30% of the asymptomatic elderly population, and recent longitudinal studies have shown that this neuropathology is associated with faster rates of cognitive decline and brain atrophy than in age-matched elderly persons with negative amyloid scans (*43–46*). Recently, it has been proposed that, for research purposes such as early intervention studies, biomarkers can be used to identify asymptomatic elderly persons at risk of AD (*47*). Three stages of preclinical AD have been proposed: individuals with only a positive pathology biomarker, individuals who also have a positive biomarker for neuronal damage, and individuals who have both types of positive biomarkers plus evidence of early cognitive decline but insufficient to meet the criteria for MCI. However, a preclinical diagnosis of AD should be restricted to research and therapy trials at this time, because data on the risk of progression to AD for these individuals is insufficient for clinical guidance. Many persons die with a significant amount of amyloid in the brain but no significant cognitive impairment (*44*). Data suggest that amyloid has an essential role in AD but alone does not account for the cognitive decline. Other factors, yet to be fully defined, play an important role in the development of dementia due to AD (*48*). Some identified factors that alter the clinical expression of AD pathology include coexistent cerebrovascular disease and coexistent neurodegenerative pathology related to α-synuclein, whereas cognitive reserve due to a large brain size and a high level of education have protective effects.

AMYLOID IMAGING

Pittsburgh Compound B (^{11}C-PiB)

^{11}C-PiB led the way in Aβ imaging. ^{11}C-PiB is a derivative of a fluorescent amyloid dye, thioflavin T, and has been shown to possess high affinity and high specificity for fibrillar Aβ (*1,2,49,50*). ^{11}C-PiB PET studies have shown not only a robust difference in ^{11}C-PiB retention between AD patients and age-matched controls (*3,36,51*) but also inverse correlations with glucose hypometabolism in some brain regions, as well as decreased cerebrospinal fluid $A\beta_{42}$ (*28,52*). Although Aβ burden as assessed by ^{11}C-PiB-PET does not correlate with measures of memory impairment in AD, it does correlate with memory impairment and rate of memory decline in MCI and healthy older subjects (*53,54*).

^{11}C-PiB in AD

On visual inspection, cortical retention of ^{11}C-PiB is elevated in AD, but the degree of binding is highly variable and does not correlate with the severity of dementia. The regional brain binding of ^{11}C-PiB is highest in the frontal cortex, cingulate gyrus, precuneus, striatum, parietal cortex, and lateral temporal cortex. The occipital cortex, sensorimotor cortex, and mesial temporal cortex are usually less affected (Fig. 1). The regional retention of ^{11}C-PiB reflects the regional density of Aβ plaques, as reported at autopsy (*55,56*) and as measured by quantification of immunohistochemical staining of brain slices, with a higher plaque density in the frontal cortex than in the hippocampus, consistent with previous neuropathologic and ^{11}C-PiB PET reports (*36,57*). In healthy individuals, a moderate degree of nonspecific uptake is seen in white matter.

^{11}C-PiB in Healthy Elderly

The prevalence of ^{11}C-PiB–positive healthy elderly persons increases each decade at the same rate as that reported in autopsy studies (*45*). Positive ^{11}C-PiB scans in apparently healthy persons are found in 12% of those in their 60s, 30% of those in their 70s, and at least 50% of those over 80 y of age (*36,53,58,59*). The prevalence of positive ^{11}C-PiB scans in the asymptomatic elderly population is strongly related to the presence of the ApoE-ε4 allele, carried by 27% of the general population. These persons have almost 3 times the risk of a positive ^{11}C-PiB scan if cognitively normal and a similar increase in the risk of developing AD (*45,60,61*). The retention of ^{11}C-PiB in healthy individuals is associated with a greater risk of cognitive decline and a faster rate of brain atrophy and is likely to represent preclinical AD (*53,54,58,59*).

Longitudinal studies with ^{11}C-PiB have confirmed that the rate of amyloid plaque accumulation in the brain is slow. In cognitively normal persons with a positive scan, the increase is on average 2%–3% per year and appears to be similar in MCI but then plateaus after the dementia of AD has developed (*46,51*). These rates of accumulation are consistent with a 10- to 20-y period of amyloid plaque accumulation before the development of dementia.

^{11}C-PiB in MCI

^{11}C-PiB scans are positive in 50%–60% of individuals with MCI, consistent with the percentage expected to progress to dementia due to AD over 3–5 y of follow-up (*53,62–64*). Unlike in AD, there is a correlation between ^{11}C-PiB binding and the degree of memory impairment. Follow-up studies have shown that 70% of ^{11}C-PiB–positive MCI subjects will progress to dementia due to AD over 3 y (*46,65*). Less than 10% of ^{11}C-PiB–negative MCI patients progress to a clinical diagnosis of AD, whereas about 20% of ^{11}C-PiB–negative MCI subjects progress to another type of dementia such as dementia with Lewy bodies or frontotemporal dementia (*46*).

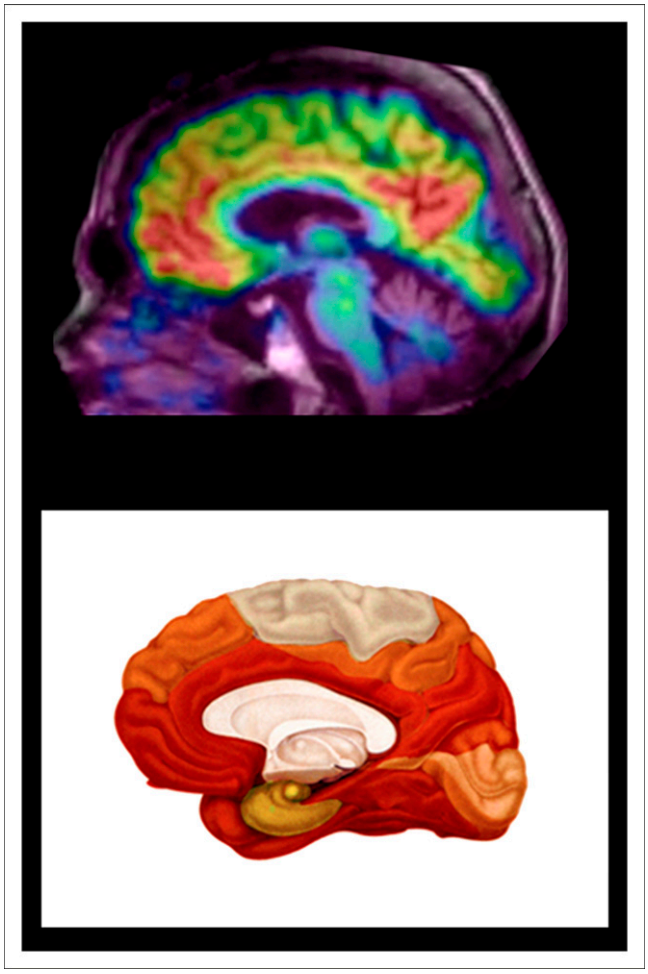

FIGURE 1. Comparison of ^{11}C-PiB PET with postmortem distribution of amyloid plaques. (Top) Representative midsagittal PET image shows regional uptake of ^{11}C-PiB overlaid on MRI, reflecting Aβ plaque burden in brain of participant with AD. (Bottom) Schematic drawing demonstrates stage C of Aβ deposition in human brain as described by Braak and Braak based on postmortem study of 2,700 brains (*16*). There is excellent concordance, with marked ^{11}C-PiB binding in frontal and anterior cortex, posterior cingulate gyrus, and precuneus (posterior medial parietal), with relative sparing of sensorimotor and occipital regions.

^{11}C-PiB in Other Conditions

Amyloid is also found in 50%–70% of patients with dementia with Lewy bodies but not in patients with frontotemporal dementia (Fig. 2) (*36*). A variable degree of AD pathology is found in many cases of clinically diagnosed vascular dementia, and it is likely that both pathologic processes contribute to the clinical presentation.

^{11}C-PiB is also elevated in subjects diagnosed with cerebral amyloid angiopathy (*66,67*), showing a distribution similar to that in AD patients except that slightly greater binding may be seen in the occipital cortex.

^{11}C-PiB studies in both asymptomatic and symptomatic persons carrying a gene mutation known to cause early-onset, autosomal-dominant familial AD have shown cortical and subcortical binding. In contrast to the retention

pattern observed in sporadic AD, individuals with mutations within the amyloid precursor protein or presenilin 1 genes associated with familial AD present with high ^{11}C-PiB retention in the striatum preceding the accumulation of amyloid plaques and ^{11}C-PiB binding in the cortical areas affected in typical sporadic AD (*68–70*).

Reading of ^{11}C-PiB Scans

Most studies to date have quantified ^{11}C-PiB binding using the cerebellar gray matter as a reference region. There is usually, but not always, far less dense amyloid plaque in the cerebellum, making it a suitable reference region for nonspecific cortical binding. Under circumstances in which there may be plaque in the cerebellum, the pons is used as the reference region. Such circumstances may include familial AD and cases of late-stage AD with advanced dementia. Under most circumstances, the ratio of cortical to cerebellar binding provides a reliable measure of brain amyloid burden. This ratio is measured after the binding in cortex and reference region achieve an apparent steady state 40–50 min after injection (*36*). The ratio is usually described as the standardized uptake value (SUV) ratio for the neocortex or a particular region. The regions for neocortical SUV ratio usually include only the cortical areas known to accumulate amyloid plaque (frontal, lateral and medial parietal, and lateral temporal cortex; anterior and posterior cingulate gyrus). The scan acquisition time is usually 20 or 30 min. Some centers prefer a dynamic scan acquired over 60 or 90 min from the time of injection in order to calculate binding using the Logan graphical method to provide a distribution volume ratio. Although this has some advantages, most groups have reported an excellent correlation between SUV ratio and distribution volume ratio, and dynamic acquisition is neither practical nor necessary for clinical practice. However, it may be appropriate for longitudinal research studies, as the test–retest variability is slightly lower and distribution volume ratio is less likely to be influenced by changes in cerebral blood flow over time. The upper limit of normal binding varies according to the size and placement of cortical and reference regions of interest but is between 1.3 and 1.6 for neocortical SUV ratio and slightly lower for distribution volume ratio.

^{11}C-PiB scans can be reliably interpreted by visual inspection, with binding at least equal to white matter uptake clearly seen in cortex, though usually this binding is clearly in excess of white matter uptake. A commonly used technique is to set a color scale on the cerebellar white matter and then inspect the midsagittal slice for uptake in the orbitofrontal cortex and posterior medial parietal area (precuneus and posterior cingulate gyrus). Transaxial slices are then reviewed for uptake in lateral temporal, parietal, and striatal regions. Interpretation of scans as positive on visual inspection correlates well with the SUV ratio cutoff for a positive scan determined in the same laboratory (*35*), though in some cases in which the cortical uptake is focal, visual inspection can be more sensitive.

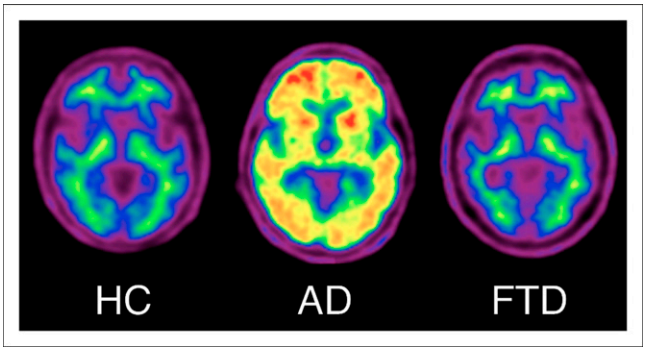

FIGURE 2. ^{18}F-florbetaben PET images of healthy aging (HC), AD, and frontotemporal dementia (FTD). ^{18}F-florbetaben images show nonspecific white matter retention in healthy elderly individual, cortical and striatal binding in patient with AD, but no cortical binding in patient with frontotemporal dementia.

^{18}F-LABELED RADIOPHARMACEUTICALS FOR AMYLOID IMAGING

Three ^{18}F-labeled radioligands for brain amyloid are in advanced stages of clinical development. These are florbetaben (*4,8,9*), florbetapir (*5,6*), and flutemetamol (*7*). All aim to provide a reliable assessment of brain amyloid with a single scan of 15- to 20-min duration. The optimal delay from injection to commencement of scan acquisition based on achieving maximal contrast between cortex and reference region (i.e., cortical SUV ratio) in AD subjects is 50 min for florbetapir and 80–90 min for florbetaben and flutemetamol. White matter uptake is greater for all 3 radiopharmaceuticals than for ^{11}C-PiB. In AD patients, the average cortical binding is similar to or less than the uptake in white matter, in contrast to ^{11}C-PiB, which shows uptake about 30% higher in cortex than in white matter. This greater white matter uptake requires a modified approach to reading images obtained with these ^{18}F-labeled amyloid tracers.

Reading ^{18}F-Amyloid Ligand Scans

The ^{11}C-PiB approach to scan interpretation frequently gives a clear answer with the ^{18}F-labeled ligands, as shown in Figures 2 and 3. This approach consists of setting a color scale that has a good dynamic range to the cerebellar white matter or pons; examining the midline sagittal slice for binding in the medial orbitofrontal cortex, cingulate gyrus, and precuneus; and examining transverse slices for frontal, parietal, lateral temporal, occipital, and striatal binding. Great care must be taken that the brain is perfectly orientated for the sagittal slice, because if this is slightly oblique, it will cut into white matter and could be mistaken for cortical binding. In a negative scan, the midline sagittal slice will clearly show the corpus callosum and pons, whereas on the transverse slices the typical white matter pattern will be seen, with more marked uptake in the perithalamic area. In a negative scan, there should be clear separation of activity between the hemispheres apart from

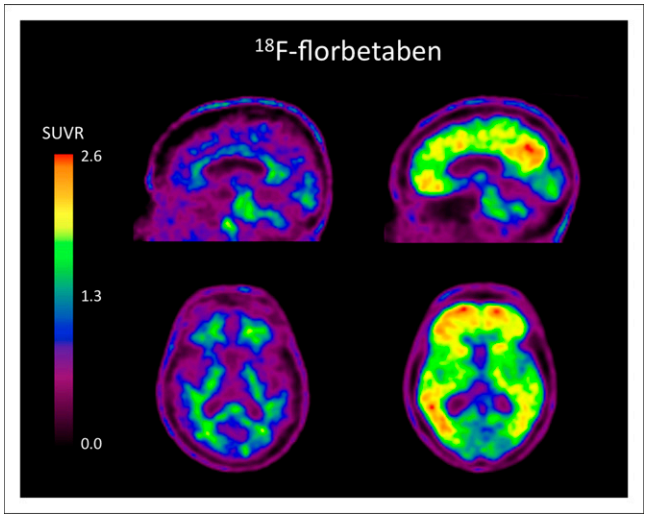

FIGURE 3. ^{18}F-florbetaben images of 2 elderly subjects with MCI. Scan on left is negative for brain amyloid. Uptake in corpus callosum and pons is clearly seen on midsagittal image and only in white matter on transverse slice. This subject remained cognitively stable over 2 y of follow-up. Scan on right is positive for brain amyloid, with binding in frontal cortex, posterior cingulate gyrus, precuneus, and lateral temporal cortex. This subject progressed to AD over 2 y of follow-up. SUVR = SUV ratio.

the white matter connections, as can be especially seen in the medial orbitofrontal and precuneus areas.

In some patients, a more sensitive approach for reading ^{18}F-amyloid scans will be needed. For this, a black-on-white background scale may be optimal, with intensity set to the global brain. The emphasis then becomes one of detecting loss of the normal white matter pattern, as binding to amyloid in the cortex will obscure the gray matter–white matter junction. A negative brain ^{18}F-amyloid scan shows a distinctive pattern of binding in white matter. In contrast, in a positive scan, uptake in cortical gray matter obscures the normal white matter pattern and shows binding extending to the outer edge of the brain, as illustrated in Figure 4.

Head movement resulting in blurring of the image will lessen the accuracy of the ^{18}F-amyloid ligands. In uncooperative patients, a thermoplastic head restraint may lessen this problem if tolerated by the patient. Severe cortical atrophy will also make image interpretation more difficult. In such circumstances, correlation with structural imaging (CT or MRI) may assist by revealing atrophy and sulcal widening that can give cortical binding an appearance similar to white matter binding.

Accuracy of Amyloid Imaging

The increasing prevalence of positive amyloid scans with advancing age in asymptomatic individuals has implications for the diagnostic accuracy of these scans for AD in patients presenting with suspected dementia. Almost all patients with AD have a positive scan (*45,71*), though a negative scan in a 91-y-old man with clinical features and cerebrospinal fluid markers of AD but only diffuse plaques postmortem has

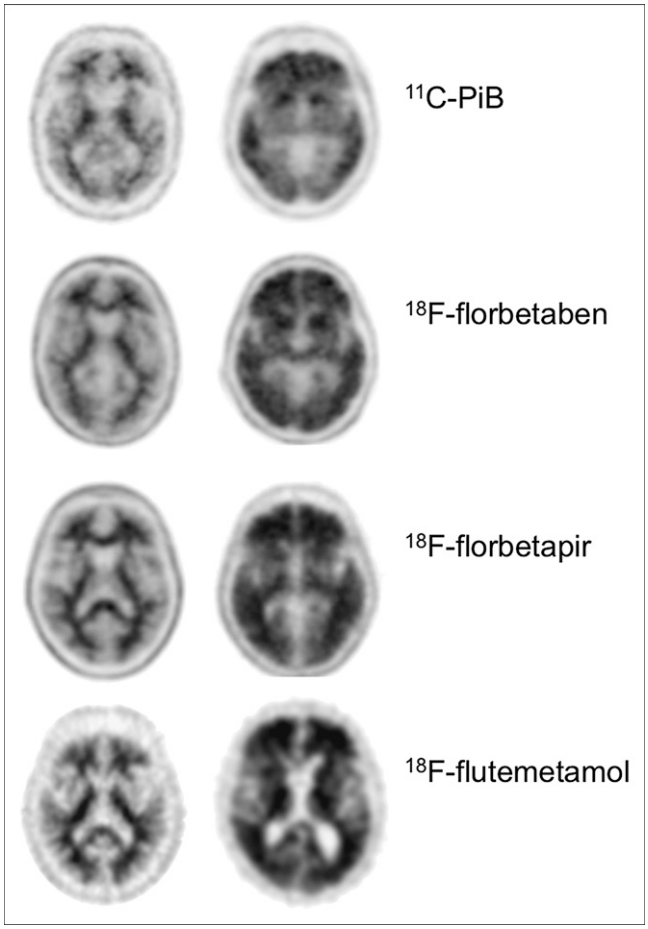

FIGURE 4. ^{11}C-PiB, ^{18}F-florbetaben, ^{18}F-florbetapir, and ^{18}F-flutemetamol images of healthy subjects and AD patients. Images on left are negative for brain amyloid and show distinctive pattern of retention in white matter. In contrast, positive scans on right illustrate that uptake in cortical gray matter obscures normal white matter pattern and that binding extends to outer edge of brain. Images were obtained from different centers (Austin Health, Avid Radiopharmaceuticals, and University of Pittsburgh) and were acquired using different cameras and reconstruction algorithms.

been reported (*72*). However, 12% of healthy persons in their 60s, 30% in their 70s, and 50% in their 80s also have a positive ^{11}C-PiB scan (*45,46,58*). It is not yet clear if these figures will also apply to the ^{18}F-amyloid ligands. Based on the ^{11}C-PiB figures, the sensitivity and negative predictive value remain high, but specificity and positive predictive value decline with age. The result is that the accuracy of amyloid imaging for AD should be over 90% for patients under the age of 70 y, about 85% for patients in their 70s, and 75%–80% for those over 80 y. Of course, if the question is "does this person have AD-related pathology?" rather than "is this patient's current clinical presentation due to AD?" the accuracy of amyloid imaging remains high at all ages, as there have been no reports of false-positive scans, when compared with histopathologic findings, and false-negative scans appear to be rare (*55–57,72*). In a report to the Food and Drug Administration on the results of a florbetapir phase

III trial with comparison to postmortem findings in 35 subjects, 9 readers had a mean accuracy of 94% for detecting significant amyloid defined as greater than sparse plaques on histopathologic examination (*71*).

Early reports suggest that the strong predictive value of a positive ^{11}C-PiB scan for progression from MCI to AD (70% over 3 y vs. <10% if ^{11}C-PiB–negative) is also seen with the ^{18}F-labeled ligands. Reports from several multicenter longitudinal studies that include cohorts with MCI will be available in the next few years to confirm or refute these early reports.

Amyloid plaques are not present in frontotemporal dementia. Several studies have shown that amyloid imaging distinguishes clinically diagnosed frontotemporal dementia from AD with high accuracy (*9,36,73–75*).

FUTURE REQUIREMENTS

To ensure wide acceptance by the clinical community, it will be necessary for all readers of amyloid scans to be trained to a high level of consistency and accuracy. This training will likely be provided by the manufacturers of ^{18}F-labeled amyloid ligands and by organizations such as the Society of Nuclear Medicine. The exact technique that provides both the highest accuracy compared with postmortem findings and consistency between readers is still under development by the developers of the ^{18}F-amyloid radiopharmaceuticals. Software programs to aid the clinical interpretation of scans are also under development. Studies of management impact and patient outcome will also likely be necessary if reimbursement is to be obtained from the government and insurers. The full potential value of amyloid imaging awaits the development of an effective therapy to slow, halt, or reverse the disease process. Such a therapy will be most beneficial when given early, before dementia has developed. Biomarkers such as amyloid imaging make development of these therapies feasible.

ACKNOWLEDGMENT

This work was funded in part by NHMRC grants 509166 and 1011689.

REFERENCES

1. Mathis CA, Bacskai BJ, Kajdasz ST, et al. A lipophilic thioflavin-T derivative for positron emission tomography (PET) imaging of amyloid in brain. *Bioorg Med Chem Lett.* 2002;12:295–298.
2. Klunk WE, Wang Y, Huang GF, et al. The binding of 2-(4′-methylaminophenyl) benzothiazole to postmortem brain homogenates is dominated by the amyloid component. *J Neurosci.* 2003;23:2086–2092.
3. Klunk WE, Engler H, Nordberg A, et al. Imaging brain amyloid in Alzheimer's disease with Pittsburgh compound-B. *Ann Neurol.* 2004;55:306–319.
4. Rowe CC, Ackerman U, Browne W, et al. Imaging of amyloid beta in Alzheimer's disease with ^{18}F-BAY94-9172, a novel PET tracer: proof of mechanism. *Lancet Neurol.* 2008;7:129–135.
5. Wong DF, Rosenberg PB, Zhou Y, et al. In vivo imaging of amyloid deposition in Alzheimer disease using the radioligand ^{18}F-AV-45 (florbetapir F 18). *J Nucl Med.* 2010;51:913–920.
6. Clark CM, Schneider JA, Bedell BJ, et al. Use of florbetapir-PET for imaging beta-amyloid pathology. *JAMA.* 2011;305:275–283.
7. Vandenberghe R, Van Laere K, Ivanoiu A, et al. ^{18}F-flutemetamol amyloid imaging in Alzheimer disease and mild cognitive impairment: a phase 2 trial. *Ann Neurol.* 2010;68:319–329.
8. Barthel H, Gertz HJ, Dresel S, et al. Cerebral amyloid-beta PET with florbetaben (^{18}F) in patients with Alzheimer's disease and healthy controls: a multicentre phase 2 diagnostic study. *Lancet Neurol.* 2011;10:424–435.
9. Villemagne VL, Ong K, Mulligan RS, et al. Amyloid imaging with ^{18}F-florbetaben in Alzheimer disease and other dementias. *J Nucl Med.* 2011;52:1210–1217.
10. Jicha GA, Parisi JE, Dickson DW, et al. Neuropathologic outcome of mild cognitive impairment following progression to clinical dementia. *Arch Neurol.* 2006;63:674–681.
11. Johnson N, Davis T, Bosanquet N. The epidemic of Alzheimer's disease: how can we manage the costs? *Pharmacoeconomics.* 2000;18:215–223.
12. Rinne JO, Brooks DJ, Rossor MN, et al. ^{11}C-PiB PET assessment of change in fibrillar amyloid-beta load in patients with Alzheimer's disease treated with bapineuzumab: a phase 2, double-blind, placebo-controlled, ascending-dose study. *Lancet Neurol.* 2010;9:363–372.
13. Jellinger KA, Bancher C. Neuropathology of Alzheimer's disease: a critical update. *J Neural Transm Suppl.* 1998;54:77–95.
14. Masters CL. Neuropathology of Alzheimer's disease. In: Burns A, O'Brien J, Ames D, eds. *Dementia.* 3rd ed. London, U.K.: Hodder Arnold; 2005:393–407.
15. Braak H, Braak E. Staging of Alzheimer-related cortical destruction. *Int Psychogeriatr.* 1997;9(suppl 1):257–261.
16. Braak H, Braak E. Frequency of stages of Alzheimer-related lesions in different age categories. *Neurobiol Aging.* 1997;18:351–357.
17. Arriagada PV, Growdon JH, Hedley-Whyte ET, Hyman BT. Neurofibrillary tangles but not senile plaques parallel duration and severity of Alzheimer's disease. *Neurology.* 1992;42:631–639.
18. Näslund J, Haroutunian V, Mohs R, et al. Correlation between elevated levels of amyloid beta-peptide in the brain and cognitive decline. *JAMA.* 2000;283:1571–1577.
19. McLean CA, Cherny RA, Fraser FW, et al. Soluble pool of Aβ amyloid as a determinant of severity of neurodegeneration in Alzheimer's disease. *Ann Neurol.* 1999;46:860–866.
20. Masters CL, Cappai R, Barnham KJ, Villemagne VL. Molecular mechanisms for Alzheimer's disease: implications for neuroimaging and therapeutics. *J Neurochem.* 2006;97:1700–1725.
21. Hardy JA, Higgins GA. Alzheimer's disease: the amyloid cascade hypothesis. *Science.* 1992;256:184–185.
22. Hardy J. Amyloid, the presenilins and Alzheimer's disease. *Trends Neurosci.* 1997;20:154–159.
23. Tanzi RE, Bertram L. New frontiers in Alzheimer's disease genetics. *Neuron.* 2001;32:181–184.
24. McKhann G, Drachman D, Folstein M, Katzman R, Price D, Stadlan EM. Clinical diagnosis of Alzheimer's disease: report of the NINCDS-ADRDA Work Group under the auspices of Department of Health and Human Services Task Force on Alzheimer's Disease. *Neurology.* 1984;34:939–944.
25. Knopman DS, DeKosky ST, Cummings JL, et al. Practice parameter: diagnosis of dementia (an evidence based review)—report of the Quality Standards Subcommittee of the American Academy of Neurology. *Neurology.* 2001;56:1143–1153.
26. McKhann GM, Knopman DS, Chertkow H, et al. The diagnosis of dementia due to Alzheimer's disease: recommendations from the National Institute on Aging-Alzheimer's Association workgroups on diagnostic guidelines for Alzheimer's disease. *Alzheimers Dement.* 2011;7:263–269.
27. Clark CM, Davatzikos C, Borthakur A, et al. Biomarkers for early detection of Alzheimer pathology. *Neurosignals.* 2008;16:11–18.
28. Fagan AM, Mintun MA, Mach RH, et al. Inverse relation between in vivo amyloid imaging load and cerebrospinal fluid Abeta(42) in humans. *Ann Neurol.* 2006;59:512–519.
29. Jack CR Jr, Knopman DS, Jagust WJ, et al. Hypothetical model of dynamic biomarkers of the Alzheimer's pathological cascade. *Lancet Neurol.* 2010;9:119–128.
30. Shaw LM, Korecka M, Clark CM, Lee VM, Trojanowski JQ. Biomarkers of neurodegeneration for diagnosis and monitoring therapeutics. *Nat Rev Drug Discov.* 2007;6:295–303.
31. de Leon MJ, Convit A, DeSanti S, et al. Contribution of structural neuroimaging to the early diagnosis of Alzheimer's disease. *Int Psychogeriatr.* 1997;9:183–190.
32. Killiany RJ, Gomez-Isla T, Moss M, et al. Use of structural magnetic resonance imaging to predict who will get Alzheimer's disease. *Ann Neurol.* 2000;47:430–439.
33. Xu Y, Jack CR Jr, O'Brien PC, et al. Usefulness of MRI measures of entorhinal cortex versus hippocampus in AD. *Neurology.* 2000;54:1760–1767.
34. Silverman DH, Small GW, Chang CY, et al. Positron emission tomography in evaluation of dementia: regional brain metabolism and long-term outcome. *JAMA.* 2001;286:2120–2127.

35. Ng S, Villemagne VL, Berlangieri S, et al. Visual assessment versus quantitative assessment of ^{11}C-PIB PET and ^{18}F-FDG PET for detection of Alzheimer's disease. *J Nucl Med.* 2007;48:547–552.
36. Rowe CC, Ng S, Ackermann U, et al. Imaging beta-amyloid burden in aging and dementia. *Neurology.* 2007;68:1718–1725.
37. Petersen RC, Smith GE, Waring SC, Ivnik RJ, Tangalos EG, Kokmen E. Mild cognitive impairment: clinical characterization and outcome. *Arch Neurol.* 1999; 56:303–308.
38. Petersen RC. Mild cognitive impairment: transition between aging and Alzheimer's disease. *Neurologia.* 2000;15:93–101.
39. Dubois B, Feldman HH, Jacova C, et al. Revising the definition of Alzheimer's disease: a new lexicon. *Lancet Neurol.* 2010;9:1118–1127.
40. Albert MS, Dekosky ST, Dickson D, et al. The diagnosis of mild cognitive impairment due to Alzheimer's disease: Recommendations from the National Institute on Aging-Alzheimer's Association workgroups on diagnostic guidelines for Alzheimer's disease. *Alzheimers Dement.* 2011;7:270–279.
41. Petersen RC, Stevens JC, Ganguli M, Tangalos EG, Cummings JL, DeKosky ST. Practice parameter: early detection of dementia: mild cognitive impairment (an evidence-based review). Report of the Quality Standards Subcommittee of the American Academy of Neurology. *Neurology.* 2001;56:1133–1142.
42. Petersen RC. Mild cognitive impairment: current research and clinical implications. *Semin Neurol.* 2007;27:22–31.
43. Price JL, Morris JC. Tangles and plaques in nondemented aging and "preclinical" Alzheimer's disease. *Ann Neurol.* 1999;45:358–368.
44. Bennett DA, Schneider JA, Arvanitakis Z, et al. Neuropathology of older persons without cognitive impairment from two community-based studies. *Neurology.* 2006;66:1837–1844.
45. Rowe CC, Ellis KA, Rimajova M, et al. Amyloid imaging results from the Australian Imaging, Biomarkers and Lifestyle (AIBL) study of aging. *Neurobiol Aging.* 2010;31:1275–1283.
46. Villemagne VL, Pike KE, Chetelat G, et al. Longitudinal assessment of Abeta and cognition in aging and Alzheimer disease. *Ann Neurol.* 2011;69:181–192.
47. Sperling RA, Aisen PS, Beckett LA, et al. Toward defining the preclinical stages of Alzheimer's disease: recommendations from the National Institute on Aging-Alzheimer's Association workgroups on diagnostic guidelines for Alzheimer's disease. *Alzheimers Dement.* 2011;7:280–292.
48. Masters CL, Beyreuther K. Alzheimer's centennial legacy: prospects for rational therapeutic intervention targeting the Abeta amyloid pathway. *Brain.* 2006; 129:2823–2839.
49. Lockhart A, Ye L, Judd DB, et al. Evidence for the presence of three distinct binding sites for the thioflavin T class of Alzheimer's disease PET imaging agents on beta-amyloid peptide fibrils. *J Biol Chem.* 2005;280:7677–7684.
50. Ye L, Morgenstern JL, Gee AD, Hong G, Brown J, Lockhart A. Delineation of positron emission tomography imaging agent binding sites on beta-amyloid peptide fibrils. *J Biol Chem.* 2005;280:23599–23604.
51. Nordberg A. Amyloid imaging in Alzheimer's disease. *Curr Opin Neurol.* 2007; 20:398–402.
52. Fagan AM, Roe CM, Xiong C, Mintun MA, Morris JC, Holtzman DM. Cerebrospinal fluid tau/beta-amyloid(42) ratio as a prediction of cognitive decline in nondemented older adults. *Arch Neurol.* 2007;64:343–349.
53. Pike KE, Savage G, Villemagne VL, et al. Beta-amyloid imaging and memory in non-demented individuals: evidence for preclinical Alzheimer's disease. *Brain.* 2007;130:2837–2844.
54. Villemagne VL, Pike KE, Darby D, et al. Abeta deposits in older non-demented individuals with cognitive decline are indicative of preclinical Alzheimer's disease. *Neuropsychologia.* 2008;46:1688–1697.
55. Bacskai BJ, Frosch MP, Freeman SH, et al. Molecular imaging with Pittsburgh compound B confirmed at autopsy: a case report. *Arch Neurol.* 2007;64:431–434.
56. Ikonomovic MD, Klunk WE, Abrahamson EE, et al. Post-mortem correlates of in vivo PiB-PET amyloid imaging in a typical case of Alzheimer's disease. *Brain.* 2008;131:1630–1645.
57. Leinonen V, Alafuzoff I, Aalto S, et al. Assessment of beta-amyloid in a frontal cortical brain biopsy specimen and by positron emission tomography with carbon 11-labeled Pittsburgh compound B. *Arch Neurol.* 2008;65:1304–1309.
58. Mintun MA, Larossa GN, Sheline YI, et al. [^{11}C]PIB in a nondemented population: potential antecedent marker of Alzheimer disease. *Neurology.* 2006;67:446–452.
59. Aizenstein HJ, Nebes RD, Saxton JA, et al. Frequent amyloid deposition without significant cognitive impairment among the elderly. *Arch Neurol.* 2008;65:1509–1517.
60. Strittmatter WJ, Saunders AM, Schmechel D, et al. Apolipoprotein E: high-avidity binding to beta-amyloid and increased frequency of type 4 allele in late-onset familial Alzheimer disease. *Proc Natl Acad Sci USA.* 1993;90:1977–1981.
61. Reiman EM, Chen K, Liu X, et al. Fibrillar amyloid-beta burden in cognitively normal people at 3 levels of genetic risk for Alzheimer's disease. *Proc Natl Acad Sci USA.* 2009;106:6820–6825.
62. Kemppainen NM, Aalto S, Wilson IA, et al. PET amyloid ligand [^{11}C]PIB uptake is increased in mild cognitive impairment. *Neurology.* 2007;68:1603–1606.
63. Price JC, Klunk WE, Lopresti BJ, et al. Kinetic modeling of amyloid binding in humans using PET imaging and Pittsburgh compound-B. *J Cereb Blood Flow Metab.* 2005;25:1528–1547.
64. Forsberg A, Engler H, Almkvist O, et al. PET imaging of amyloid deposition in patients with mild cognitive impairment. *Neurobiol Aging.* 2008;29:1456–1465.
65. Okello A, Koivunen J, Edison P, et al. Conversion of amyloid positive and negative MCI to AD over 3 years: an ^{11}C-PIB PET study. *Neurology.* 2009;73:754–760.
66. Johnson KA, Gregas M, Becker JA, et al. Imaging of amyloid burden and distribution in cerebral amyloid angiopathy. *Ann Neurol.* 2007;62:229–234.
67. Ly JV, Donnan GA, Villemagne VL, et al. ^{11}C-PIB binding is increased in patients with cerebral amyloid angiopathy-related hemorrhage. *Neurology.* 2010; 74:487–493.
68. Klunk WE, Price JC, Mathis CA, et al. Amyloid deposition begins in the striatum of presenilin-1 mutation carriers from two unrelated pedigrees. *J Neurosci.* 2007;27:6174–6184.
69. Koivunen J, Verkkoniemi A, Aalto S, et al. PET amyloid ligand [^{11}C]PIB uptake shows predominantly striatal increase in variant Alzheimer's disease. *Brain.* 2008;131:1845–1853.
70. Villemagne VL, Ataka S, Mizuno T, et al. High striatal amyloid beta-peptide deposition across different autosomal Alzheimer disease mutation types. *Arch Neurol.* 2009;66:1537–1544.
71. FDA Advisory Committee Briefing Document: NDA #202-008—Florbetapir F18 Injection. U.S. Food and Drug Administration Web site. http://www.fda.gov/downloads/AdvisoryCommittees/CommitteesMeetingMaterials/Drugs/PeripheralandCentralNervousSystemDrugsAdvisoryCommittee/UCM240266.pdf.
72. Cairns NJ, Ikonomovic MD, Benzinger T, et al. Absence of Pittsburgh compound B detection of cerebral amyloid beta in a patient with clinical, cognitive, and cerebrospinal fluid markers of Alzheimer disease: a case report. *Arch Neurol.* 2009;66:1557–1562.
73. Drzezga A, Grimmer T, Henriksen G, et al. Imaging of amyloid plaques and cerebral glucose metabolism in semantic dementia and Alzheimer's disease. *Neuroimage.* 2008;39:619–633.
74. Engler H, Santillo AF, Wang SX, et al. In vivo amyloid imaging with PET in frontotemporal dementia. *Eur J Nucl Med Mol Imaging.* 2008;35:100–106.
75. Rabinovici GD, Furst AJ, O'Neil JP, et al. ^{11}C-PIB PET imaging in Alzheimer disease and frontotemporal lobar degeneration. *Neurology.* 2007;68:1205–1212.

Journal of NUCLEAR MEDICINE TECHNOLOGY

Brain Amyloid Imaging

Christopher C. Rowe and Victor L. Villemagne

J. Nucl. Med. Technol. 2013;41:11-18.
Published online: February 8, 2013.
Doi: 10.2967/jnumed.110.076315

Journal of Nuclear Medicine Technology is published quarterly.
SNMMI | Society of Nuclear Medicine and Molecular Imaging
1850 Samuel Morse Drive, Reston, VA 20190.
(Print ISSN: 0091-4916, Online ISSN: 1535-5675)

SNMMI SOCIETY OF NUCLEAR MEDICINE AND MOLECULAR IMAGING